[1]*Peiman Esmaeili

[2]Rahmatollah Mirzaei

Fuzzy Output Feedback Control for Interleaved Floating Dual Boost Converter (IFDBC) Interfacing DC Microgrid with Constant Power Load

Journal of Electrical Systems

Abstract: - The present investigation aimed to develop a novel fuzzy output feedback control strategy for interleaved floating dual boost converters (IFDBC) interfaced DC microgrid with a constant power load. In this study, a hybrid fuzzy controller in tandem with a non-linear observer was proposed to mitigate the adverse effects of constant power loads on the system's stability, thereby ensuring large-signal stability and reducing voltage undershoot and overshoot. Furthermore, the proposed controller was designed to enhance the system's response speed and robustness against various disturbances. The primary focus of this study was the simulation of the proposed IFDBC converter fed by a constant current source, which is representative of a constant power load. The results demonstrate that the overall performance of the system exhibits satisfactory behavior against gradually applied changes and disturbances, with reliable outcomes. Moreover, the proposed structure is not only suitable for high-power loads, but also applicable for loads with low and limited power that are highly sensitive to voltage fluctuations, where even small changes in voltage can significantly impact their performance.

Keywords: Fuzzy control, DC microgrid, Boost converter, Constant power load

I. INTRODUCTION

IFDB converter has been proposed to simultaneously obtain high voltage gain and high-power operation capability [1], [2]. Both input and output current and voltage ripple are suppressed thanks to their interconnected structure, allowing the use of small-sized inductors and capacitors to increase system power density and increase system reliability. Power electronic loads are increasingly used in modern direct current microgrids [3], [4]. Since the power electronic loads with tight adjustment may change quickly in the sense of a large signal in a transient time, they are called constant power loads for simplicity in this study. The stability of the DC microgrid is seriously threatened since the constant power loads show the characteristics of negative incremental impedance and nonlinearity [5], [6]. Thus, the control of interleaved converters, such as IFDBC, becomes a challenging issue to ensure the stability of DC microgrid systems.

Many control strategies have been proposed in recent years to meet the increasing requirements of DC microgrid stabilization with constant power loads. These control strategies can be classified into linear approaches and non-linear approaches [7-18]. Among the linear approaches, the passive damping method is extensively used to increase the stability of the system. Negative incremental impedance can be fully compensated by introducing passive components into the system [19]. However, passive damping methods introduce additional physical components such as capacitors and resistors, which increase system costs and power losses. Some active damping methods have been presented to avoid these disadvantages. The primary idea of active damping is to inject virtual impedance to shape the loop gain of the system and achieve system stability. In [20], virtual impedance is injected into the source converter to maintain the dominant poles of the system in the left half of the complex plane. A source-side series virtual impedance control method has been presented in [21].

To solve the control problems expressed in modern power networks, fuzzy logic controllers are often preferred as an alternative approach [22]. Fuzzy logic systems possess a straightforward and comprehensible structure, making them an attractive solution for various applications. The widespread adoption of fuzzy logic in both commercial and laboratory settings is a testament to its effectiveness. Furthermore, the incorporation of fuzzy logic into control systems can lead to enhanced machine control and cost savings. While the accuracy of fuzzy logic outputs may be subject to limitations, the acceptable results obtained can be utilized with confidence, owing to the system's reliability and robustness [23]. In the present study, an IFDBC converter was used to provide low voltage and current ripple in addition to high power gain. Also, among the well-known nonlinear control methods, fuzzy logic control is considered an effective method in the control of nonlinear systems [24]-[44]. Given what was stated, the present study was conducted to control the fuzzy output feedback for IFDBC with a constant power load.

[1] [1]Master of Electrical Engineering - Power Electronics and Electrical Machines, University of Kurdistan, Sanandaj, Iran

[2]Associate Professor, Dept. of Electrical Engineering, Engineering Faculty, University of Kurdistan, Sanandaj, Iran

* Corresponding author

II. METHODS

The basic configuration of a fuzzy system consists of a fuzzifier, some fuzzy if-then rules, a fuzzy inference engine and a defuzzifier. The Mamdani-type fuzzy system [45] has been widely used in the modeling and control of nonlinear systems [46]-[52]. The control objective of this section is to construct an adaptive fuzzy feedback controller $u(t)$ to ensure that all closed-loop system signals remain bounded and the system output $y_i(t)$ meets the desired reference signals $y_{mi}(t)$ with performance constraints prescribed for $e_i(t) = y_{mi}(t) - y_i(t), i = 1, \dots, p$ tracking errors are slow. To quantify the prescribed performance limits, the tracking errors e_i must satisfy the inequalities in relation (1-2) [53], [54], [55].

$$-\delta_i \mu_i(t) < e_i(t) < \bar{\delta}_i \mu_i(t), \quad i = 1, \dots, p \tag{1-2}$$

where δ_i and $\bar{\delta}_i$ are positive constants, $\mu_i(t) : R^+ \to R^+/\{0\}$ with $\lim_{t\to\infty} \mu_i(t) = \mu_{i\infty} > 0$ is a positive decreasing smooth function, named as a performance function, which is set as: $\mu_i(t) = (\mu_{i0} - \mu_{i\infty})e^{-k_i t} + \mu_{i\infty}$, with $\mu_{i0} > \mu_{i\infty} > 0$ and $k_i > 0$.

In the fuzzy system, the lth fuzzy rule is written as follows, $R^{(l)}: IF \;\; x_1 \;\; is \;\; F_1^l \;\; and \dots and \;\; x_n \;\; is F_n^l, \;\; then \;\; y \;\; is \;\; G^l$, that F_i^l and G^l are fuzzy sets that are related to the fuzzy membership $\mu_{F_i^l}(x_i)$ and $\mu_{G^l}(y)$, respectively. $l = 1, 2, \dots, m$ and m is equal to the number of general rules. The terms, $x = [x_{r_1 1}, \cdots, x_{r_1 r_1}, \cdots, x_{r_p 1}, \cdots, x_{r_p r_p}]^T$, $u = [u_1, \cdots, u_p]^T \in R^p \; and \; y = [y_1, \cdots, y_p]^T \in R^p$ are the state vector, input vector and output vector of system, respectively.

By using singleton fuzzification strategy, product inference and central average defuzzification, the output of the fuzzy system is presented in the form of equation (2-2)

$$y(x) = \frac{\sum_{l=1}^{m} y^l (\prod_{i=1}^{n} \mu_{F_i^l}(x_i))}{\sum_{l=1}^{m} \prod_{i=1}^{n} \mu_{F_i^l}(x_i)} \tag{2-2}$$

where $y^l = max_{y \in R} \mu_{G^l}(y)$.

In this study, we design the following controller based on [56]

$$u = R\hat{s}u_0 \tag{3-2}$$

$$\dot{\hat{s}} = v - R[F(x) + G(x, u^*)u + D(t)] + RX_r \tag{4-2}$$

where $X_r = [\dot{x}_{r_1 r_1} - \dot{\hat{x}}_{r_1 r_1}, \dots, \dot{x}_{r_p r_p} - \dot{\hat{x}}_{r_p r_p}]$, $\tilde{\dot{x}} = [\dot{\hat{x}}_{r_1 1} - \dot{x}_{r_1 1}, \dots, \dot{\hat{x}}_{r_1 r_1} - \dot{x}_{r_1 r_1}, \dots, \dot{\hat{x}}_{r_p 1} - \dot{x}_{r_p 1}, \dots, \dot{\hat{x}}_{r_p r_p} - \dot{x}_{r_p r_p}]$, $D(t) = [d_1(t), \cdots, d_p(t)]^T$, $d_i(t), i = 1, 2, \cdots, p$ are the external disturbance of system, and $F_i(x, u), i = 1, 2, \cdots, p$ are Lipschitz continuous unknown smooth nonlinear functions and it is assumed that only the output vector y is measurable. according to study, $F_i(x, u)$, can be approximated by fuzzy systems.

The sign of the matrix $G(x, u^*)$ is unknown, and thus, a Nussbaum-type function technique can be employed to estimate the unknown sign. Specifically, a function $N(\zeta)$ is deemed a Nussbaum-type function if it satisfies the following properties:

$$\lim_{s\to+\infty} \sup \frac{1}{s} \int_0^s N(\zeta) d\zeta = +\infty \tag{5-2}$$

$$\lim_{s\to+\infty} \inf \frac{1}{s} \int_0^s N(\zeta) d\zeta = -\infty \tag{6-2}$$

Substituting equation (3-2) into equation (4-2), which is equal to the derivative of the filtered transformed error estimate, we will have

$$\dot{\hat{s}} = v - R[F(x) + G(x, u^*)R\hat{s}u_0 + D(t)] + RX_r \tag{7-2}$$

Finally, the controller u_0 can be designed in the form of relations (8-2) and (9-2)

$$u_0 = -\lambda_0 N(\zeta) \Upsilon^2 \tag{8-2}$$

$$\dot{\zeta} = \lambda_0 \|R\hat{s}\|^2 \Upsilon^2 \tag{9-2}$$

where $N(\zeta) = \exp(\zeta^2)\cos(\frac{\pi}{2}\zeta)$ and λ_0 is a positive constant value.

In this equations $\Upsilon = \|R^{-1}v\| + \frac{1}{2}\|R^{-1}\hat{s}\| + \sum_{i=1}^{p}\|\theta_{f_i}\|\|\xi_{f_i}(\hat{x})\| + 2\|R\hat{s}\|$, $\dot{\theta}_{f_i} = -\eta_{f_i}(\hat{s}_i\gamma_i\|\xi_{f_i}(\hat{x})\| + l_{f_i}\theta_{f_i})$, $v_i = [0, \Lambda_i^T]\hat{E}_i + \varrho_{r_i}^i\left(e_i, \dot{\hat{e}}_i, \dots, \hat{e}_i^{(r_i-1)}, t\right) + \gamma_i y_{mi}^{(r_i)}$, $R = \text{diag}[\gamma_1, \dots, \gamma_p]$ and $\gamma_i = \frac{\frac{\bar{\delta}_i+\delta_i}{2}}{\mu_i\left(\bar{\delta}_i - \frac{e_i}{\mu_i}\right)\left(\delta_i + \frac{e_i}{\mu_i}\right)}$.

Noted that $\Lambda_i = [\bar{\lambda}_{i1}, \dots, \bar{\lambda}_{ir_i-1}]$ is properly chosen such that $s^{r_i-1} + \bar{\lambda}_{ir_i-1}s^{r_i-2} + \cdots + \bar{\lambda}_{i1}$ is Hurwitz, ξ_{f_i} is m-dimensional row vector in Euclidean space with $0 < \xi^T(x)\xi(x) \leq 1$ [59] and η_{f_i} and l_{f_i} are positive constants.

The obtained control system is applied to the desired IFDBC converter. In order to simplify the equations and reduce the circuit parameters and according to [7], because the inductors in different phases have the same inductance due to the symmetry of the system and using the same duty ratio ($u_i = u_{m1}\ for\ i = 1, 2, \dots, N/2$) with proper phase shift to generate PWM switching signal for each phase, a generalized reduced order model of N-phase IFDB converter can be written as equation (10-2).

$$\begin{aligned} L_{eq}\frac{di_{in1,2}}{dt} &= \left[v_{in} - (1 - u_{m1,2})v_{c1,2}\right] \\ C_{1,2}\frac{di_{in1,2}}{dt} &= \left[i_{in1,2}(1 - u_{m1,2}) - i_{out}\right] \end{aligned} \tag{10-2}$$

where $i_{in1,2} = [i_{in1} = \sum_{i=1}^{N/2} i_{Li}, i_{in2} = \sum_{i=N/2+1}^{N} i_{Li}]$, $u_{m1,2}$, $v_{c1,2}$, $C_{1,2}$ and i_{out} are input currents to the upper and lower modules, the control inputs of the upper and lower modules, the voltage of the capacitors of the upper and lower modules, the capacitors of the upper and lower and the output current (load) respectively. It should be mentioned that in this relation, $L_{eq} = 2L/N$, is the equivalent inductance of input side.

III. RESULTS

System assumptions

Table 1 shows the circuit characteristics of the system used in the study. In this study, the values of all inductors will be $L_{eq} = [L_{eq1}, L_{eq2}]$, all capacitors will be $C = [C_1, C_2]$ and all control inputs will be $u = [u_1, u_2]$.

Table 1: Parameters of IFDBC converter

Parameter	*Symbol*	*Value*	*Unit of measurement*
input voltage	v_{in}	100	V
Inductor	L_{eq}	2.33	mH
capacitor	C	1410	μF
Load capacity	P_{CPL}	60	kW
Switching frequency	f_s	20	kHz
Control input	$\boldsymbol{u}$		

The novel IFDB converter architecture has been streamlined according to the equation (10-2) and is depicted in Figure 1. The distinguishing feature of this design is the inclusion of an additional diode, D_{tr}, in parallel with the inductor and primary diode of the circuit. This modification is aimed at mitigating the impact of high starting currents, which can otherwise compromise the integrity of the desired circuit components. The operation of this diode is designed to ensure that it conducts only during the start-up phase, when the voltage on the load side is lower than that on the source side. Once the voltage on the load side exceeds that on the source side, entering the permanent mode, the diode acts as an open circuit and does not interfere with the continued operation of the circuit. This simplified structure has demonstrated improved performance and control system efficiency.

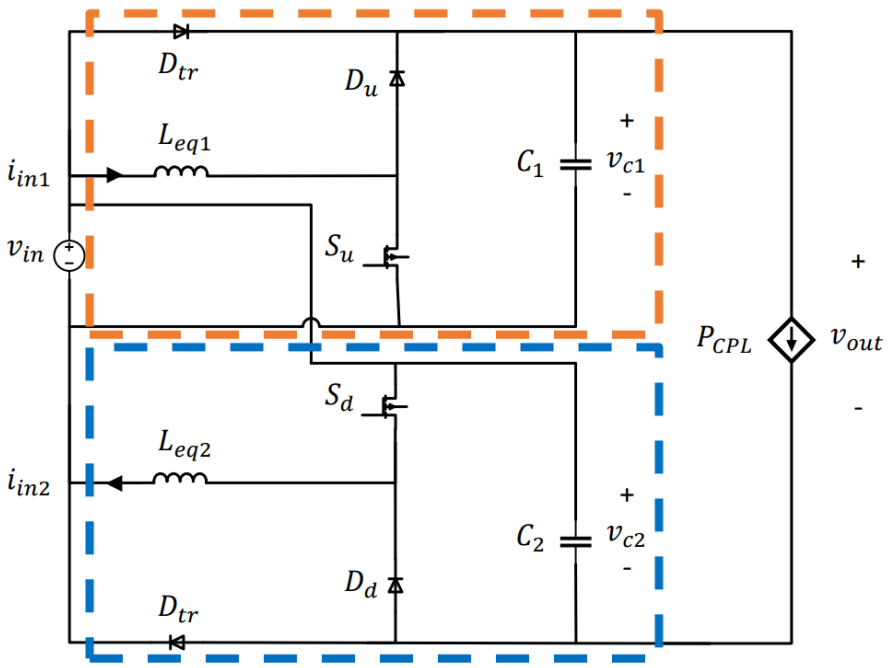

Figure 1: Circuit schematic of the simulated system

Table 2 shows the parameters of the fuzzy controller system.

Table 2: Parameters of the controller system in the system with IFDB converter

μ_{10}, μ_{20}	0.1	l_{F1}, l_{F2}	0.1
$\mu_{1\infty}, \mu_{2\infty}$	0.1	l_{f1}, l_{f2}	0.01
$\overline{\delta}_1, \underline{\delta}_1$	4.8	Λ_1, Λ_2	1.5
$\overline{\delta}_2, \underline{\delta}_2$	4.8	λ_0	0.002
k_1, k_2	1	f	[1,1]
$\theta_{F1}(0), \theta_{F2}(0)$	0.5	H	[44000,44000]
$\theta_{f1}(0), \theta_{f2}(0)$	0.1	A	-[44000,44000]
$\zeta(0)$	1	Q	1000
η_{F1}, η_{F2}	1.5	P	22000
η_{f1}, η_{f2}	0.5	V_{ref}	300

System response to load power changes

Step changes in load power

As shown in Figure 2, the system has reached the value determined for the reference voltage $v_{ref} = 300V$, indicating the correct and fast operation of the controller and the appropriateness of the selected parameter values. In this section, the output voltage overshoot of the system was about 350V and the system reached its constant and optimal value in less than 0.01 seconds. Also, the currents i_{L1} and i_{L2} shown in Figure 2 indicate the optimal performance of the system in controlling the inrush current in the transient moments of the system. It should be noted that the amount of inrush and inrush of currents i_{L1} and i_{L2} were about 270A and 250A, respectively. These current values, according to the capacity of the converter and the control system, will not cause damage to the circuit and the control system.

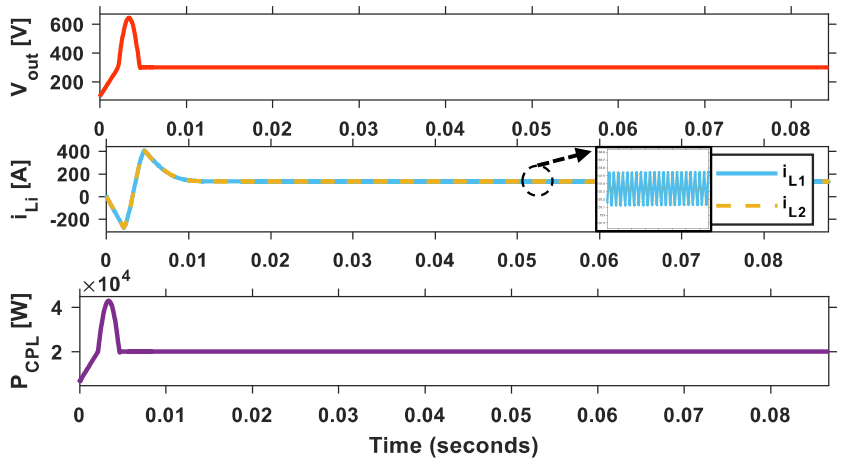

Figure 2: Controller performance in convergence to the reference voltage value

Also in Figure 3, The control inputs fluctuate around its average value which is 0.5. The amplitude of this fluctuation is about 0.2. The simulation and how to change this amplitude will be discussed.

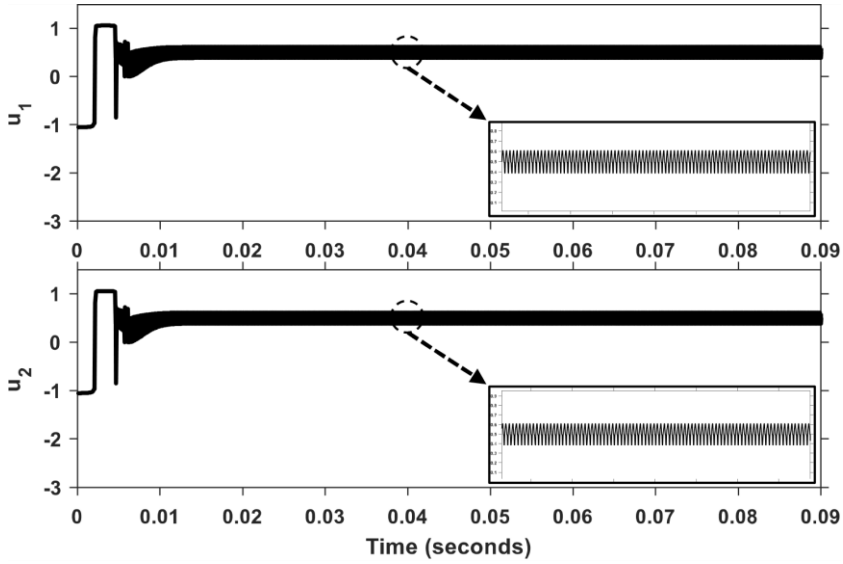

Figure 3: Changes in control inputs u_1 and u_2 in convergence to the reference voltage value

In the continuation of this section, the performance of the system in the presence of load changes and disturbances has been discussed in the form of steps. In this regard, a constant power load is applied to the system in steps of 20, 40, and 60kW, respectively, to check the response of the system to this scenario.

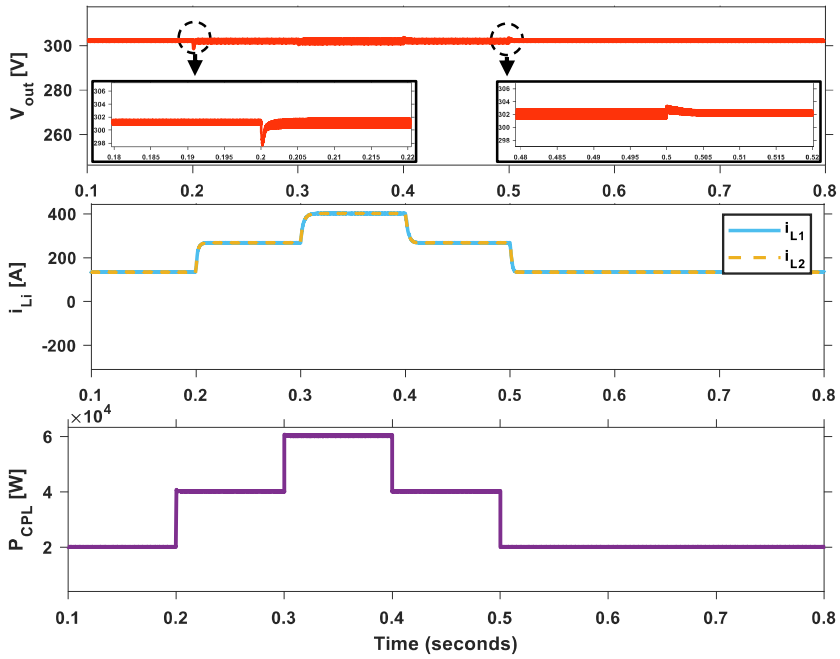

Figure 4: The control system response to the step load changes applied to the system with the IFDB converter

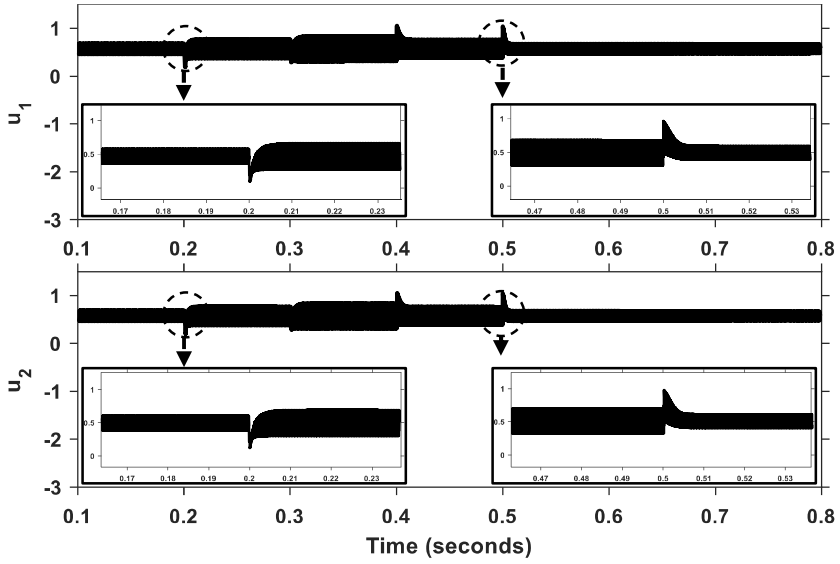

Figure 5: Changes in control inputs u_1 and u_2 in the presence of power step changes in the system with IFDB converter

As shown in Figure 4, the constant power load is adjusted at 20, 40, 60, 40, and 20kW at the moments of 0.2, 0.3, 0.4, and 0.5 seconds, respectively, so the system performance in the modes that may occur to the system is shown. According to Figure 4, the output voltage of the system with a maximum jump of 4V and the inductor-currents i_{L1} and i_{L2} also reaching their new value without any overshoot or undershoot in less than 0.005 seconds, indicating the fast operation of the control system.

Also, the control inputs are shown in Figure 5 and as it is known, at the moments of 0.3 and 0.4 seconds with Considering the high load power of P_{CPL} and the inductor-currents i_{L1} and i_{L2}, the range of changes of the control inputs u_1 and u_2 is larger. Nevertheless, the system has been successful in controlling the voltage.

Gradual changes in load power

As depicted in Figure 6, the system exhibits a comparable performance to the full-step mode previously discussed. Notably, the output voltage does not exhibit overshoots or undershoots, and only the amplitude of the output voltage is

modified. In this figure, prior to the 0.2-second mark, the output voltage of the system is adjusted to an amplitude of 1V and an average value of 301.5V, consistent with the previous section.

Figure 7 illustrates the control inputs, showcasing the dynamic behavior of u_1 and u_2 during transitions in the system. As observed, when the power supply is incremented to 60kW, the amplitude of control inputs u_1 and u_2 increases. However, the system successfully maintains voltage regulation.

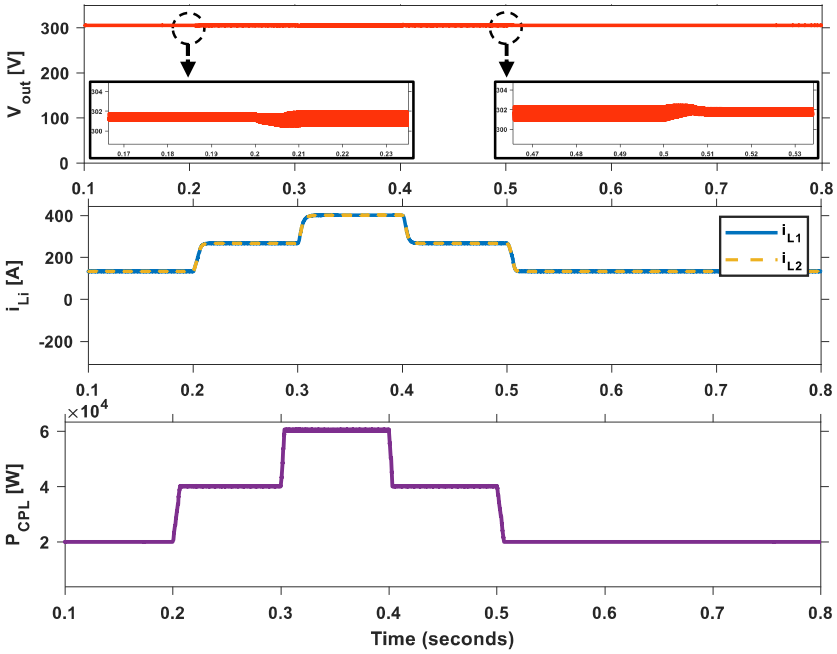

Figure 6: The control system response to the gradual changes of applied load

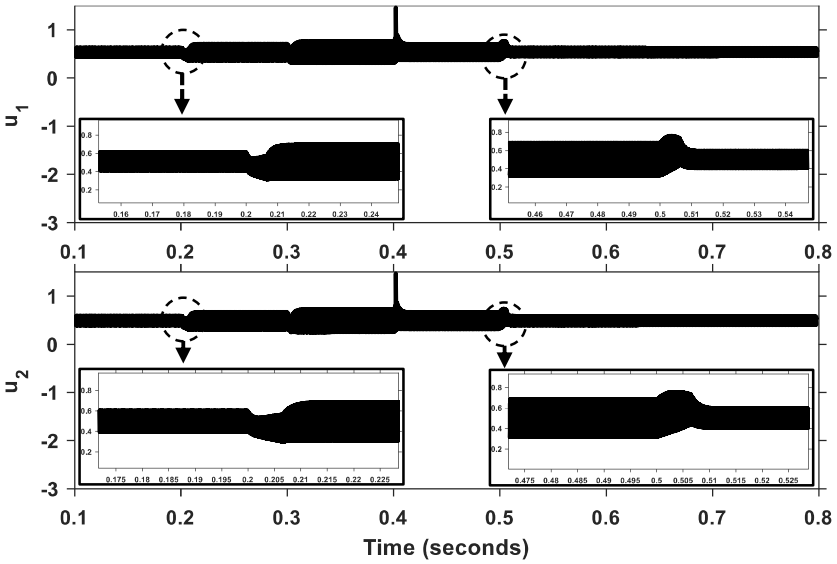

Figure 7: Changes in control inputs u_1 and u_2 in the presence of gradual power changes

System response to reference voltage changes

Step changes of the reference voltage

As depicted in Figure 8, the output voltage v_{out} exhibits a rapid settling behavior, achieving its new value within a short time frame. Specifically, the overshoot values at the instances of 0.2 and 0.3 seconds, corresponding to the step changes in the reference voltage, are approximately 20V and 40V, respectively. Notably, the output voltage achieves its new value with a predictable slope, converging within a mere 0.001 seconds.

Figure 9 illustrates the impact of reference voltage changes on control inputs u_1 and u_2. A comparative analysis with similar cases involving load changes in the previous section reveals that the effect of reference voltage changes on

power quality and output voltage stability is significantly more pronounced than that of load power changes. Consequently, the changes in inductor currents and control inputs are substantial.

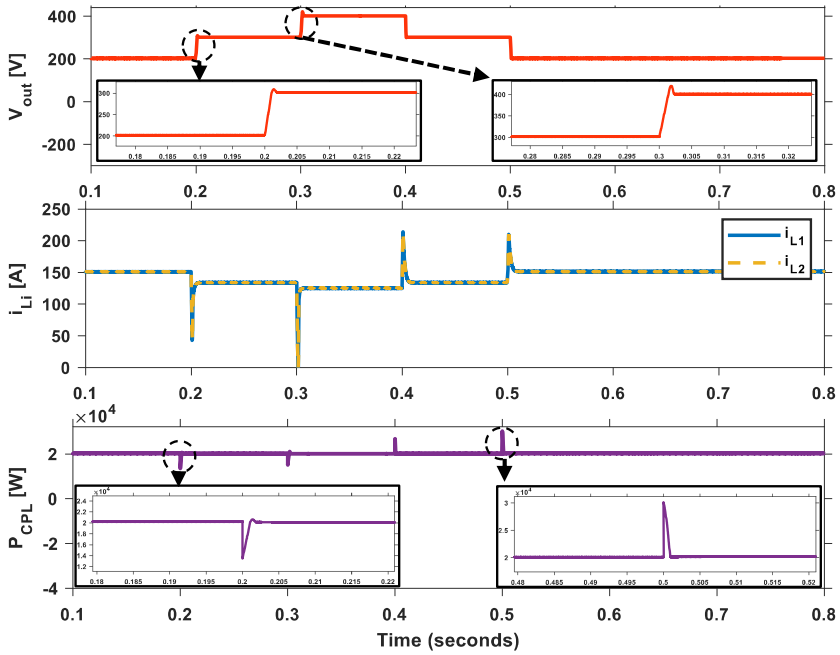

Figure 8: The control system response to step changes in the reference voltage

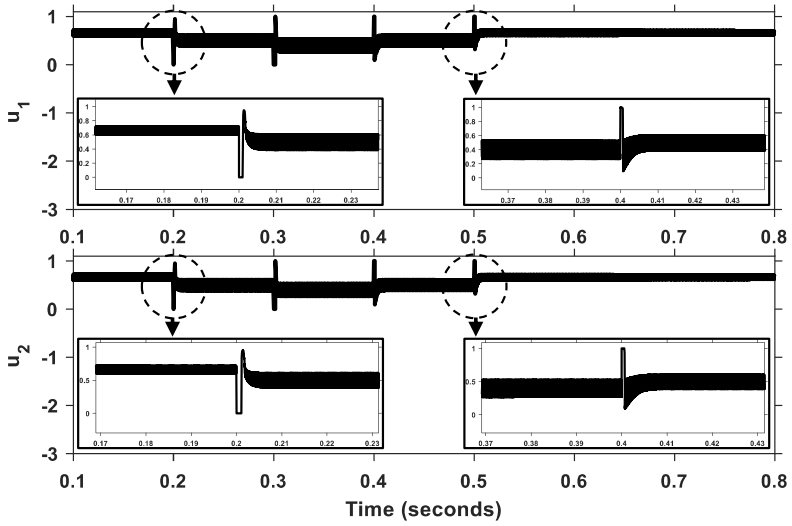

Figure 9: Changes in control inputs u_1 and u_2 in the presence of step changes in reference voltage

Gradual changes in the reference voltage

As shown in Figure 10, the output voltage v_{out} has reached its new value according to the determined slope and without overshoot and undershoot in its value. The undershoot values at the moments of 0.2 and 0.3 seconds were about 6A and 35A, respectively. Also, the overshoot values at the moments of 0.4 and 0.5 seconds were about 20A and 7A, respectively, indicating that the inductor currents in the state of gradual change of the reference voltage compared to the state of a step change of the reference voltage due to its lower slope has less overshoot and undershoot. Figure 11 also shows the effects of reference voltage changes on control inputs u_1 and u_2.

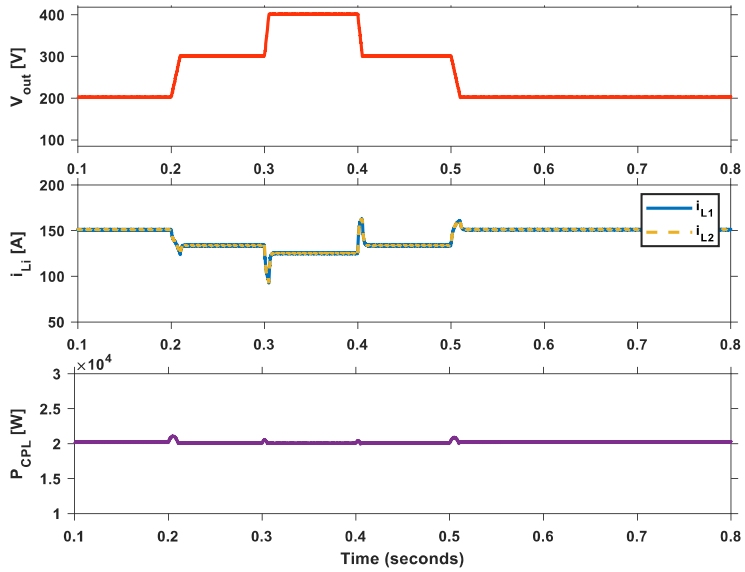

Figure 10: The control system in the presence of gradual changes in the reference voltage

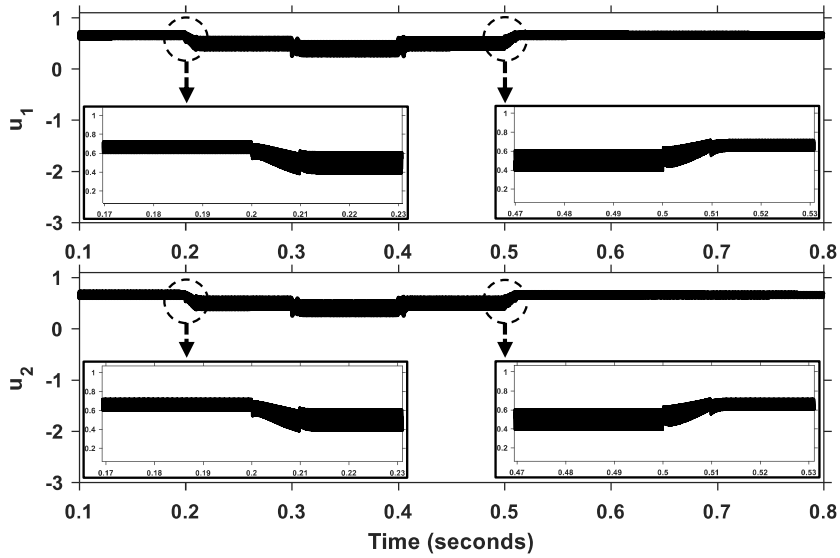

Figure 11: Changes in the control inputs u_1 and u_2 in the presence of gradual changes in the reference voltage

System response to input voltage changes

Step changes in input voltage

As shown in Figure 12, at the moment of 0.2 seconds when the system input voltage increases, the control system reacts quickly, and by changing the control inputs u_1 and u_2, the inductor currents i_{L1} and i_{L2} decrease. Also, at the moment of 0.3 seconds, when the system experiences a severe voltage drop of 18%, the system correctly increases the inductor currents of i_{L1} and i_{L2} by changing the control inputs u_1 and u_2. Also, the control inputs u_1 and u_2 will change due to these scenarios, as shown in Figure 13.

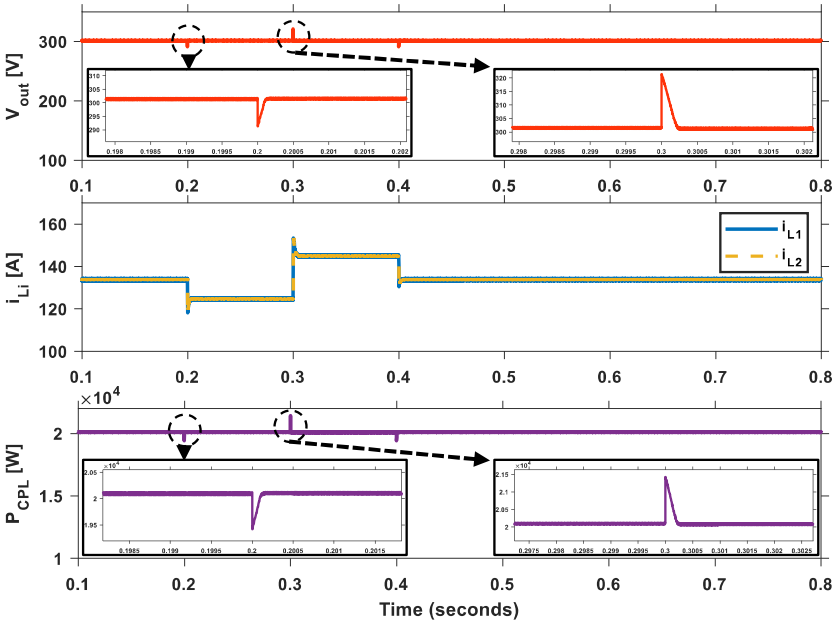

Figure 12: The control system response to step changes in the input voltage

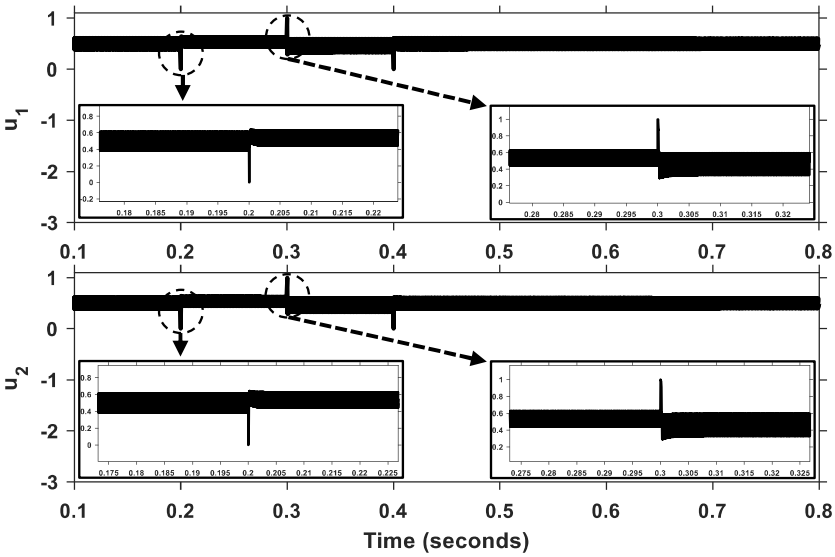

Figure 13: Changes in control inputs u_1 and u_2 in the presence of step changes in input voltage

Gradual changes in input voltage

As shown in Figure 14, the output voltage has been fixed at the moment of 0.2 seconds without significant change in its amplitude and only with a slight increase of 0.2V in its average value. Also, due to the 18% decrease in the input voltage at the moment of 0.3 seconds, the output voltage amplitude remains approximately constant, and its average value is fixed with a decrease of 0.3V. Figure 15 shows how control inputs change due to applied scenarios. The control system may undergo rapid and small changes in moments that are quickly resolved. Since the used control is of the fuzzy type, such occurrences can be expected.

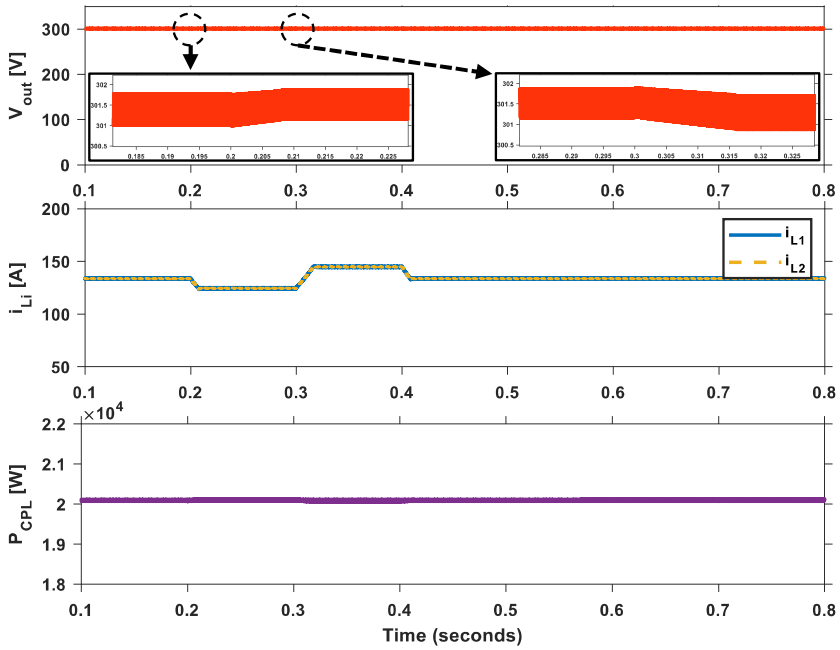

Figure 14: The control system response to the gradual changes in the input voltage

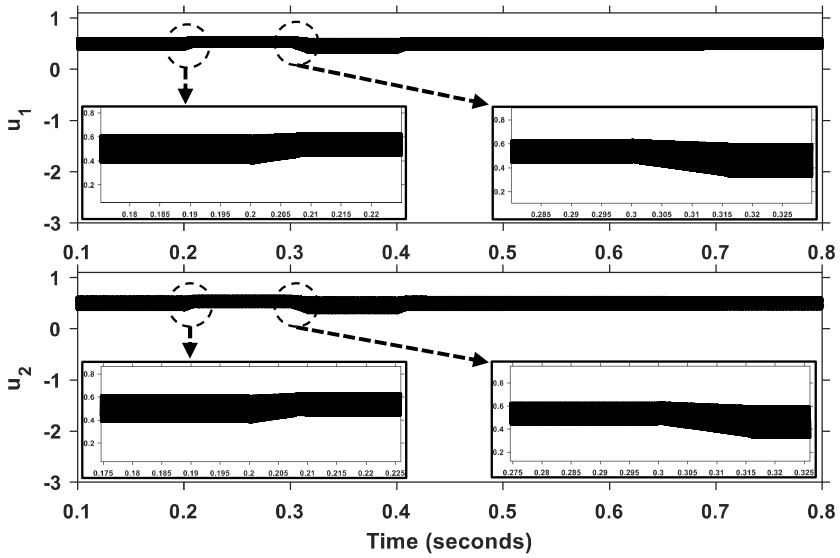

Figure 15: Changes in control inputs u_1 and u_2 in the presence of gradual changes in input voltage

System response to parameter changes

Based on [57], the IFDB converter is naturally resistant to parametric uncertainties, and the changes included in the section related to the boost converter will have very little effect on the system output with the boost converter as the interleave between load and energy sources. In this simulation, different parametric scenarios have been applied to the system with an IFDB converter. Figure 16 shows the dynamic response of DC voltage with parametric uncertainties (state 1: $L_1 = L_2 = 1.2L$ and $C_1 = C_2 = C$; state 2: $L_1 = L_2 = 0.8L$, $C_1 = 1.1C$, and $C_2 = 0.9C$; state 3: $L_1 = L_2 = 0.8L$ and $C_1 = C_2 = 1.1C$; state 4: $L_1 = L_2 = 1.2L$, $C_1 = 0.9C$, and $C_2 = 1.1C$; state 5: $L_1 = L_2 = L$ and $C_1 = C_2 = C$) under the condition of 10 increase in the microgrid input. The results show that the converter is resistant to parameter uncertainties.

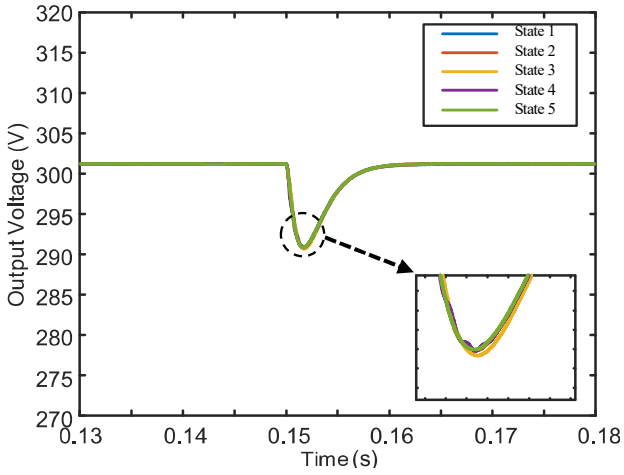

Figure 17: Performance of the system with IFDB converter against parametric uncertainties

Comparison with the sliding-mode control (SMC) method

This section compares this research with the sliding-mode control presented in [57] for the final review and comparison of the microgrid system and the control method presented in the previous sections. By investigating the changes in voltage and inductor currents related to each of the fuzzy and sliding-mode methods in Figure 18 as a result of changing the power of the constant power load, it can be seen that both controllers show appropriate and fast performance in the face of these changes. However, undershoots of about 20V in the output voltage and overshoots of about 35A are observed in the inductor currents of the system with the sliding-mode controller.

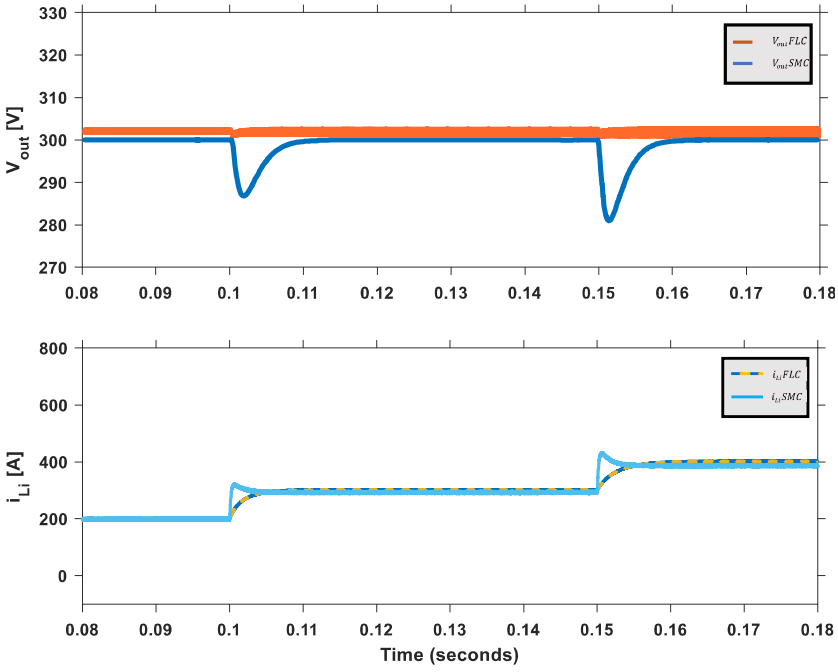

Figure 18: Comparing the performance of fuzzy control and sliding-mode control in the presence of constant power load changes

Figure 19 depicts the oscillations in the output voltage and inductor currents resulting from the implementation of the sliding-mode controller and the new proposed control strategy. Specifically, the figure shows maximum overshoots of approximately 22V and 10A, respectively, and maximum undershoots of approximately 13V and 22A, respectively.

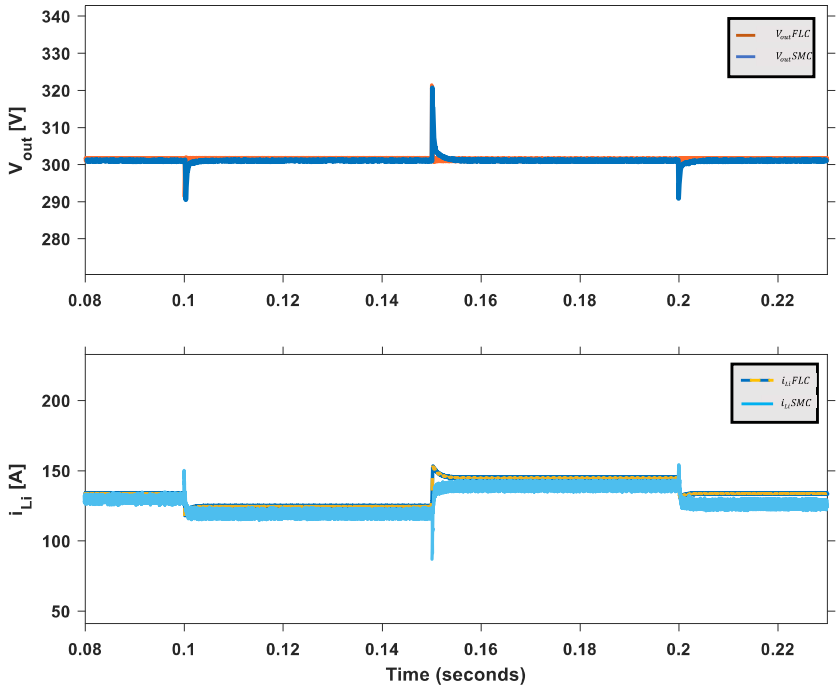

Figure 19: Comparing the performance of fuzzy control and sliding-mode control in the presence of microgrid input voltage changes

In Figure 20, undershoots at about 10V in the output voltage and overshoots and undershoots of about 270A and 130A, respectively, are seen in the inductor currents of the system with the sliding-mode controller. Based on the investigations, it can be concluded that the performance of the presented microgrid system with fuzzy control was very suitable and compared to sliding mode control has provided similar, and in some cases, better performance under the same conditions, despite knowing that it might have inaccurate results.

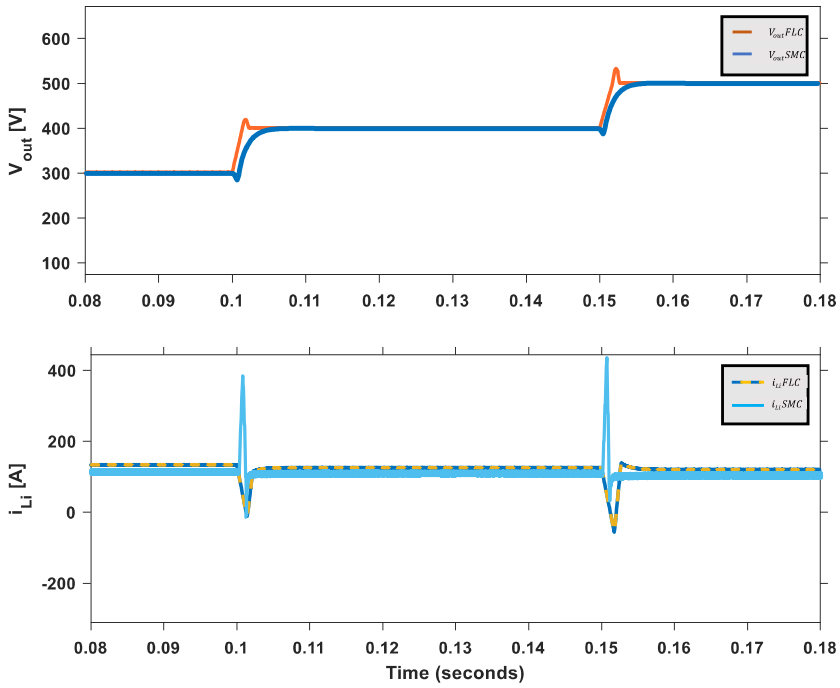

Figure 20: Comparing the performance of fuzzy control and sliding-mode control in the presence of microgrid reference voltage changes

IV. CONCLUSION

The simulation results demonstrate the efficacy of the control method in accurately tracking the signal and maintaining the measured error within the specified range. The controller's performance was evaluated in the context of a boost converter, subjected to a variety of scenarios that may occur in the system. These scenarios included step and gradual changes in load power, reference voltage, and input voltage, as well as step changes in the size of the inductor and capacitor. Furthermore, a parallel diode was added to the current flow path in the inductor to regulate the initial inrush current.

The simulation results unequivocally demonstrate the controller's ability to provide fast and standard performance in the face of these diverse scenarios. Notably, significant reductions in overshoots and undershoots of the output voltage were observed, compared to other control methods. The stability of the microgrid system is ensured by the controller's robust performance, which is characterized by its ability to effectively mitigate disturbances and maintain a stable output voltage.

REFERENCES

[1] F. S. Garcia, J. A. Pomilio, G. Spiazzi et al., "Modeling and control design of the interleaved double dual boost converter." IEEE Trans. Ind. Electron., vol. 60, no. 8, pp. 3283–3290, 2013.

[2] S. Choi, V. Agelidis, J. Yang, D. Coutellier, and P. Marabeas, "Analysis, design and experimental results of a floating-output interleaved-input boost-derived dc–dc high-gain transformer-less converter," IET Power Electron., vol. 4, no. 1, pp. 168–180, 2011.

[3] L. Zhang, X. Ruan, and X. Ren, "Second-harmonic current reduction for two-stage inverter with boost-derived front-end converter: Control schemes and design considerations," IEEE Trans. Power Electron., vol. 33, no. 7, pp. 6361–6378, 2017.

[4] L. Zhang and X. Ruan, "Control schemes for reducing second harmonic current in two-stage single-phase converter: An overview from dc-bus port-impedance characteristics," IEEE Trans. Power Electron., vol. 34, no. 10, pp. 10 341–10 358, 2019.

[5] Y. Zhao, W. Qiao, and D. Ha, "A sliding-mode duty-ratio controller for dc/dc buck converters with constant power loads," IEEE Trans. Ind. Appli., vol. 50, no. 2, pp. 1448–1458, 2014.

[6] M. Wu and D. D.-C. Lu, "A novel stabilization method of lc input filter with constant power loads without load performance compromise in dc microgrids," IEEE Trans. Ind. Electron., vol. 2, no. 7, pp. 4552–4562, 2015.

[7] Y. Yang and C. Zhou, "Adaptive fuzzy h/sub /spl infin// stabilization for strict-feedback canonical nonlinear systems via backstepping and small-gain approach," IEEE Transactions on Fuzzy Systems, vol. 13, no. 1, pp. 104–114, 2005.

[8] B. Chen, X. Liu, K. Liu, and C. Lin, "Direct adaptive fuzzy control of nonlinear strict-feedback systems," Automatica, vol. 45, no. 6, pp. 1530–1535, 2009.

[9] B. Chen, X. Liu, K. Liu, and C. Lin, "Fuzzy approximation-based adaptive control of nonlinear delayed systems with unknown dead zone," IEEE Transactions on Fuzzy Systems, vol. 22, no. 2, pp. 237– 248, 2014.

[10] C. Chen, z. liu, K. Xie, Y.-J. Liu, Y. Zhang, and C. L. P. Chen, "Adaptive fuzzy asymptotic control of mimo systems with unknown input coefficients via a robust nussbaum gain based approach," IEEE Transactions on Fuzzy Systems, vol. 25, no. 5, pp. 1252–1263, 2017.

[11] Y.-J. Liu, S.-C. Tong, and T.-S. Li, "Observer-based adaptive fuzzy tracking control for a class of uncertain nonlinear mimo systems," Fuzzy Sets and Systems, vol. 164, no. 1, pp. 25–44, 2011.

[12] W. Shi, R. Luo, and B. Li, "Adaptive fuzzy prescribed performance control for mimo nonlinear systems with unknown control direction and unknown dead-zone inputs," ISA Trans, vol. 66, pp. 86–95, 2017.

[13] B. Chen, X. Liu, K. Liu, and C. Lin, "Adaptive fuzzy tracking control of nonlinear mimo systems with time-varying delays," Fuzzy Sets and Systems, vol. 217, pp. 1–21, 2013.

[14] T. Zhang, M. Xia, and Y. Yi, "Adaptive neural dynamic surface control of strict-feedback nonlinear systems with full state constraints and unmodeled dynamics," Automatica, vol. 81, pp. 232–239, 2017.

[15] K. Xie, C. Chen, F. L. Lewis, and S. Xie, "Adaptive asymptotic neural network control of nonlinear systems with unknown actuator quantization," IEEE Trans Neural Netw Learn Syst, vol. 29, no. 12, pp. 6303–6312, 2018.

[16] Q. Zhou, P. Shi, Y. Tian, and M. Wang, "Approximation-based adaptive tracking control for mimo nonlinear systems with input saturation," IEEE Trans Cybern, vol. 45, no. 10, pp. 2119–2028, 2015.

[17] Z. Li, T. Li, G. Feng, R. Zhao, and Q. Shan, "Neural networkbased adaptive control for pure-feedback stochastic nonlinear systems with time-varying delays and dead-zone input," IEEE Transactions on Systems, Man, and Cybernetics: Systems, Digital Object Identifier 10.1109/TSMC.2018.2872421.

[18] T. L. Zifu Li and G. Feng, "Adaptive neural control for a class of stochastic nonlinear time-delay systems with unknown dead zone using dynamic surface technique," Int. J. Robust Nonlinear Control, vol. 26, pp. 759–781, 2016.

[19] M. Cespedes, L. Xing, and J. Sun, "Constant-power load system stabilization by passive damping," IEEE Trans. Power Electron., vol. 26, no. 7, pp. 1832–1836, 2011.
[20] A. M. Rahimi and A. Emadi, "Active damping in dc/dc power electronic converters: A novel method to overcome the problems of constant power loads," IEEE Trans. Ind. Electron., vol. 56, no. 5, pp. 1428–1439, 2009.
[21] X. Zhang, Q.-C. Zhong, V. Kadirkamanathan, J. He, and J. Huang, "Source-side series-virtual-impedance control to improve the cascaded system stability and the dynamic performance of its source converter," IEEE Trans. Power Electron., vol. 1, no. 1, pp. 1–1, 2018.
[22] P. Prabhakaran, Y. Goyal, and V. Agarwal, "Novel nonlinear droop control techniques to overcome the load sharing and voltage regulation issues in DC microgrid," IEEE Trans. Power Electron., vol. 33, no. 5, pp. 4477– 4487, May 2018.
[23] H. Wang, M. Han, R. Han, J. M. Guerrero, and J. C. Vasquez, "A decentralized current-sharing controller endows fast transient response to parallel DC-DC converters," IEEE Trans. Power Electron., vol. 33, no. 5, pp. 4362–4372, May 2018.
[24] C. P. Bechlioulis and G. A. Rovithakis, "Robust adaptive control of feedback linearizable mimo nonlinear systems with prescribed performance," IEEE Transactions on Automatic Control, vol. 53, no. 9, pp. 2090–2099, 2008.
[25] C. P. Bechlioulis and G. A. Rovithakis, "Adaptive control with guaranteed transient and steady state tracking error bounds for strict feedback systems," Automatica, vol. 45, no. 2, pp. 532–538, 2009.
[26] C. P. Bechlioulis and G. A. Rovithakis, "Prescribed performance adaptive control for multi-input multi-output affine in the control nonlinear systems," IEEE Transactions on Automatic Control, vol. 55, no. 5, pp. 1220–1226, 2010.
[27] L. Zhang, S. Tong, and Y. Li, "Prescribed performance adaptive fuzzy output-feedback control of uncertain nonlinear systems with unmodeled dynamics," Nonlinear Dynamics, vol. 77, no. 4, pp. 1653–1665, 2014.
[28] S. Sui, S. Tong, and Y. Li, "Observer-based fuzzy adaptive prescribed performance tracking control for nonlinear stochastic systems with input saturation," Neurocomputing, vol. 158, pp. 100–108, 2015.
[29] Y. Song, Y. Wang, and C. Wen, "Adaptive fault-tolerant pi tracking control with guaranteed transient and steady-state performance," IEEE Transactions on Automatic Control, vol. 62, no. 1, pp. 481–487, 2017.
[30] J. X. Zhang and G. H. Yang, "Fuzzy adaptive output feedback control of uncertain nonlinear systems with prescribed performance," IEEE Trans Cybern, vol. 48, no. 5, pp. 1342–1354, 2018.
[31] L. Zhang, Y. Li, and S. Tong, "Adaptive fuzzy output feedback control for mimo switched nonlinear systems with prescribed performances," Fuzzy Sets and Systems, vol. 306, pp. 153–168, 2017.
[32] Q. Zhou, H. Li, L. Wang, and R. Lu, "Prescribed performance observer based adaptive fuzzy control for nonstrict-feedback stochastic nonlinear systems," IEEE Transactions on Systems, Man, and Cybernetics: Systems, pp. 1747–1758, 2018.
[33] S. Tong, S. Sui, and Y. Li, "Fuzzy adaptive output feedback control of mimo nonlinear systems with partial tracking errors constrained," IEEE Transactions on Fuzzy Systems, vol. 23, no. 4, pp. 729–742, 2015.
[34] W. Shi and B. Li, "Adaptive fuzzy control for feedback linearizable mimo nonlinear systems with prescribed performance," Fuzzy Sets and Systems, vol. 344, pp. 70–89, 2018.
[35] W. Shi, F. Yan, and B. Li, "Adaptive fuzzy decentralized control for a class of nonlinear systems with different performance constraints," Fuzzy Sets and Systems, vol. 374, pp. 1–22, 2019.
[36] J. Na, Q. Chen, X. Ren, and Y. Guo, "Adaptive prescribed performance motion control of servo mechanisms with friction compensation," IEEE Transactions on Industrial Electronics, vol. 61, no. 1, pp. 486–494, 2014.
[37] E. Psomopoulou, A. Theodorakopoulos, Z. Doulgeri, and G. A. Rovithakis, "Prescribed performance tracking of a variable stiffness actuated robot," IEEE Transactions on Control Systems Technology, vol. 23, no. 5, pp. 1914–1926, 2015.
[38] C. Hua, J. Chen, and X. Guan, "Adaptive prescribed performance control of quavs with unknown time-varying payload and wind gust disturbance," Journal of the Franklin Institute, vol. 355, no. 14, pp. 6323–6338, 2018.
[39] K. P. Tee, S. S. Ge, and E. H. Tay, "Barrier lyapunov functions for the control of output-constrained nonlinear systems," Automatica, vol. 45, no. 4, pp. 918–927, 2009.
[40] K. P. Tee, B. Ren, and S. S. Ge, "Control of nonlinear systems with time-varying output constraints," Automatica, vol. 47, no. 11, pp. 2511– 2516, 2011.
[41] Y.-J. Liu, S. Lu, S. Tong, X. Chen, C. L. P. Chen, and D.-J. Li, "Adaptive control-based barrier lyapunov functions for a class of stochastic nonlinear systems with full state constraints," Automatica, vol. 87, pp. 83–93, 2018.
[42] Y.-J. Liu and S. Tong, "Barrier lyapunov functions for nussbaum gain adaptive control of full state constrained nonlinear systems," Automatica, vol. 76, pp. 143–152, 2017.
[43] Y.-J. Liu, M. Gong, S. Tong, C. L. P. Chen, and D.-J. Li, "Adaptive fuzzy output feedback control for a class of nonlinear systems with full state constraints," IEEE Transactions on Fuzzy Systems, vol. 26, no. 5, pp. 2607–2617, 2018.
[44] H. Li, S. Zhao, W. He, and R. Lu, "Adaptive finite-time tracking control of full state constrained nonlinear systems with dead-zone," Automatica, vol. 100, pp. 99–107, 2019.
[45] LX-Wang, A Course in Fuzzy Systems and Control. Prentice-Hall Inc, NewYork, 1997.

[46] A. Boulkroune, M. M'Saad, and M. Farza, "Adaptive fuzzy controller for multivariable nonlinear state time-varying delay systems subject to input nonlinearities," Fuzzy Sets and Systems, vol. 164, no. 1, pp. 45–65, 2011.
[47] W. Shi, "Adaptive fuzzy control for mimo nonlinear systems with nonsymmetric control gain matrix and unknown control direction," IEEE Transactions on Fuzzy Systems, vol. 22, no. 5, pp. 1288–1300, 2014.
[48] S. Tong and Y. Li, "Adaptive fuzzy output feedback control of mimo nonlinear systems with unknown dead-zone inputs," IEEE Transactions on Fuzzy Systems, vol. 21, no. 1, pp. 134–146, 2013.
[49] W. Shi, "Observer-based fuzzy adaptive control for multi-input multioutput nonlinear systems with a nonsymmetric control gain matrix and unknown control direction," Fuzzy Sets and Systems, vol. 263, pp. 1– 26, 2015.
[50] Y. Li, S. Tong, and T. Li, "Hybrid fuzzy adaptive output feedback control design for uncertain mimo nonlinear systems with time-varying delays and input saturation," IEEE Transactions on Fuzzy Systems, vol. 24, no. 4, pp. 841–853, 2016.
[51] Y. Li, K. Li, and S. Tong, "Finite-time adaptive fuzzy output feedback dynamic surface control for mimo nonstrict feedback systems," IEEE Transactions on Fuzzy Systems, vol. 27, no. 1, pp. 96–110, 2019.
[52] Y. Li, S. Tong, and T. Li, "Hybrid fuzzy adaptive output feedback control design for uncertain mimo nonlinear systems with time-varying delays and input saturation," IEEE Transactions on Fuzzy Systems, vol. 24, no. 4, pp. 841–853, 2016.
[53] C. P. Bechlioulis and G. A. Rovithakis, "Robust adaptive control of feedback linearizable mimo nonlinear systems with prescribed performance," IEEE Transactions on Automatic Control, vol. 53, no. 9, pp. 2090–2099, 2008.
[54] C. P. Bechlioulis and G. A. Rovithakis, "Adaptive control with guaranteed transient and steady state tracking error bounds for strict feedback systems," Automatica, vol. 45, no. 2, pp. 532–538, 2009
[55] J. Na, Q. Chen, X. Ren, and Y. Guo, "Adaptive prescribed performance motion control of servo mechanisms with friction compensation," IEEE Transactions on Industrial Electronics, vol. 61, no. 1, pp. 486–494, 2014.
[56] W. Shi, "Adaptive Fuzzy Output-Feedback Control for Nonaffine MIMO Nonlinear Systems With Prescribed Performance," in IEEE Transactions on Fuzzy Systems, vol. 29, no. 5, pp. 1107-1120, May 2021, doi: 10.1109/TFUZZ.2020.2969110.
[57] W. Jiang, X. Zhang, P. Lin, X. Zhang, H. H. C. Iu and T. Fernando, "Combined Sliding-Mode Control for the IFDBC Interleaved DC Microgrids With Power Electronic Loads," in IEEE Journal of Emerging and Selected Topics in Power Electronics, vol. 8, no. 4, pp. 3396-3410, Dec. 2020, doi: 10.1109/JESTPE.2020.2982564.